Analytical Methods

Accepted Manuscript

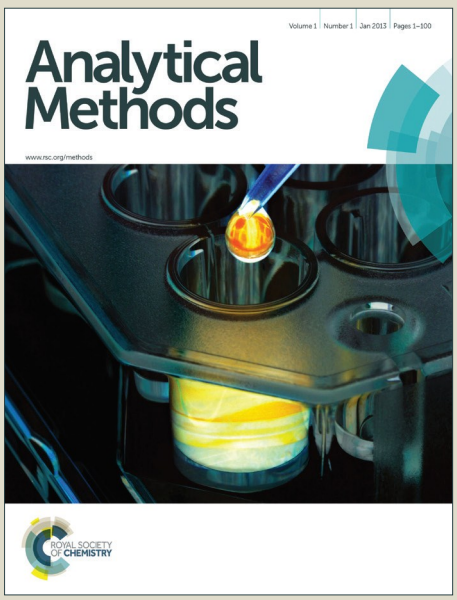

This is an *Accepted Manuscript*, which has been through the Royal Society of Chemistry peer review process and has been accepted for publication.

Accepted Manuscripts are published online shortly after acceptance, before technical editing, formatting and proof reading. Using this free service, authors can make their results available to the community, in citable form, before we publish the edited article. We will replace this *Accepted Manuscript* with the edited and formatted *Advance Article* as soon as it is available.

You can find more information about *Accepted Manuscripts* in the Information for Authors.

Please note that technical editing may introduce minor changes to the text and/or graphics, which may alter content. The journal's standard Terms & Conditions and the Ethical guidelines still apply. In no event shall the Royal Society of Chemistry be held responsible for any errors or omissions in this *Accepted Manuscript* or any consequences arising from the use of any information it contains.

ROYAL SOCIETY OF CHEMISTRY

www.rsc.org/methods

Anal. Methods

ARTICLE

Molecular imprinted polymer-based chemiluminescence imaging assay for the determination of ethopabate residue in chicken muscle†

Zhaozhou Li*, Zhili Li, Daomin Li, Hongli Gao, Xiujin Chen, Li Cao, Yuze Hou and Songbiao Li

Received 19th July 2015,
Accepted xxth xx 2015

DOI: 10.1039/x0xx00000x

www.rsc.org/

A new molecular imprinted polymer (MIP)-chemiluminescence (CL) method has been developed for the detection of ethopabate (ETP) residue in chicken muscle. The MIP microsphere was prepared using precipitation polymerization with ETP as a template, methacrylic acid as a functional monomer and pentaerythritol triacrylate as a cross-linker in the porogen of acetonitrile. The prepared MIP microspheres were characterized by the scanning electron microscope, differential scanning calorimeter and Fourier transform infrared spectrometer. The binding properties of ETP on the imprinted polymers were evaluated by the equilibrium rebinding experiment. It was revealed that two classes of the binding sites were produced in the resulting ETP MIP with the dissociation constants of 23.92 μg L^{-1} and 77.82 μg L^{-1}, and the affinity binding sites of 8808.28 μg g^{-1} and 14043.90 μg g^{-1}, respectively. As the artificial biomimetic recognition element for ETP, the polymer microspheres were immobilized in microtiter plates (96 wells) with poly(vinyl alcohol) as a glue. Through the optimizations of the MIP absorption and CL imaging conditions, ETP was quantified based on peroxyoxalate CL reaction enhanced by imidazole. Under the optimum conditions, the relative CL intensity has a linear relationship with the ETP concentration in the range of 0.1 μg mL^{-1} to 30μg mL^{-1}, with a limit of detection 14.7 μg kg^{-1} and a limit of qualification 20.4 μg kg^{-1} in chicken muscle. The recoveries of spiked ETP are in the range of 99.80%-99.98% with the relative standard deviation of 1.7%-3.4%. For the first time, the CL method combined with MIP was developed to determine trace ETP in the real sample, and the results show that it can become a useful analytical tool for quick detection in residue analysis.

Introduction

Ethopabate (ETP), methyl 4-acetamido-2-ethoxybenzoate, is a coccidiostat frequently used in the prophylaxis and treatment of coccidiosis and leukocytozoonosis in chickens. It has a synergistic effect with some other anticoccidial drugs [1]. Although the withdrawal time has been established for ETP, its residue is frequently found in products derived from poultry eggs and meat. At the present time, the application of ETP is prohibited in many countries, and the US Code of Federal Regulations (CFR) has established a maximum residue limit (MRL) of 500 μg kg^{-1} in chicken muscles and 1500 μg kg^{-1} in chicken liver [2]. Since the lack of control and legislation regarding usage and residue of veterinary drugs in food, ETP is not phased out in many developing countries. Therefore, it is worthwhile to develop reliable analytical approaches for the measurement of ETP residue in low concentration levels in chicken tissue samples.

Several analytical methods have been developed for the determination of ETP residue, such as spectrofluorimetric assay [1], gas chromatography [3], high-performance liquid chromatography (HPLC) with UV detection [4] or by fluorimetry [5], liquid chromatograph-mass spectrometry [6, 7], etc. However, the instruments of these methods are not only expensive and complicated, but are also laborious and time-consuming [8]. Accordingly, there is a considerable interest in the development of simple, rapid, economical and selective methods that will afford the analysis of samples. In recent years, chemiluminescence (CL) has become very popular due to its simple operation, high sensitivity, wide linear range, and short analysis time. But the low selectivity is the dominant factor restricting its application in complicated sample analysis.

Molecular imprinting is known as a template polymerization method, of producing "tailor-made", highly selective synthetic receptors for given molecules [9]. Owing to its high selectivity, inherent stability, low cost, and simple preparation, molecular imprinted polymers (MIPs) have already been identified as chromatographic stationary phases, enzyme mimics and sensor components with predetermined selectivity for the target molecule. By using MIPs as recognition elements, the selectivity of the CL methods can be greatly improved and most commonly present interferences can be minimized. It is reported that the molecular imprinted polymer (MIP)-based CL assay has been developed to determine the analyte in real sample [8, 10, 11]. However, the related

College of Food and Bioengineering, Henan University of Science and Technology, Luoyang 471023, P. R. China. E-mail: ilizhaozhou@126.com; Fax: +86 379 64282342; Tel: +86 379 64282342.

† Electronic Supplementary Information (ESI) available: [details of any supplementary information available should be included here]. See DOI: 10.1039/x0xx00000x

Analytical Methods Accepted Manuscript

data are still scarce, it is necessary to conduct further studies.

Currently, there is no report about using a MIP-based CL method for ETP residue analysis. The purpose of this work was to develop a selective CL imaging assay coupled with MIP for simultaneous determination of trace ETP in complicated samples. Precipitation polymerization method was used for preparing the imprinted microsphere with uniform shape. Then, microtiter plates were coated with the polymeric microspheres in place by using poly(vinyl alcohol) (PVA) as a glue. The amount of polymer- bound ETP was quantified using an imidazole (IMZ)-catalyzed peroxy-oxalate chemiluminescence (PO-CL) system. Furthermore, the light emitted by the chemiluminescent reaction was determined with a high-resolution CCD camera. The proposed method not only broadens the applicability of PO-CL system, but also presents an alternative approach for screening ETP residues in the foods of animal origin.

Experimental

Materials and reagents

ETP standard was purchased from Hubei Widely Chemical Technology Co., Ltd, China. Methyl 4-amino-2-methoxybenzoate (MAM), IMZ and hydrogen peroxide solution (H_2O_2) were obtained from Aladdin Industrial Corporation. Methyl 4-amino-2-ethoxybenzoate (MAE) was received from Hangzhou Sage Chemical Co., Ltd. Methyl-4-acetamidobenzoate (MAB) was synthesized from methyl-4-aminobenzoate. Bis (2, 4, 6-trichlorophenyl) oxalate (TCPO) was prepared as described earlier [12]. Functional monomers (methacrylic acid, MAA; acrylamide, AM; 4-vinylpyridine, 4-VP) and the cross-linker (pentaerythritol triacrylate, PETRA) were purchased from Sigma-Aldrich. Benzoyl peroxide (BPO), N, N-dimethylaniline (DMA), methanol, acetonitrile, acetic acid, hydrochloric acid, PVA and other reagents were obtained from Sinopharm Chemical Reagent Co., Ltd. Water used was filtered from a Millipore Milli-Q purification system. Chicken muscle samples were purchased from the local market.

Apparatus

An Agilent 8453 double-beam spectrophotometer was used for recording UV spectra and determining the absorbance. Microscopic morphology was examined on a field emission scanning electron microscope (JSM-6700F, JEOL Ltd., Japan), thermal stability was evaluated by a differential scanning calorimeter (Mettler-Toledo Group, Switzerland) and infrared spectra were recorded on a Digilab Fourier transform infrared spectrometer (FTS3000). Additionally, the light emitted was quantified using a PMT (operated at -600V) of the IFFL-D Chemiluminescence Analyzer (Xi'an Ruike Electronic Science Tech. Co. Ltd., China).

The determination of ETP, MAE, MAM and MAB, whose chemical structures are shown in Fig. 1, was carried out on a Varian liquid chromatographic system (Varian Company, USA) equipped with a Prostar 210 pump, a LC workstation version 6.41 system soft-ware and a Prostar 325 UV-Vis detector. Chromatographic separation was performed on a C18 reversed-phase column (5 μm, 4.6 mm ×250 mm Zorbax SB, Agilent Corporation, USA). The mobile phase consisted of 35% water and 65% methanol (by volume). Effluents were monitored at a wavelength of 268 nm. The flow rate was 1 mL min^{-1}, the injection volume was 10 μL, and the column temperature was maintained at the room temperature (22 °C).

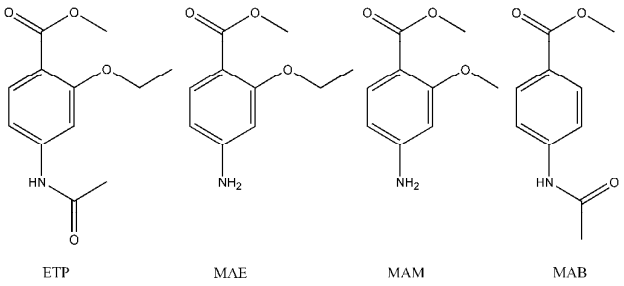

Fig. 1 Chemical structures of ethopabate (ETP), methyl 4-amino-2-methoxybenzoate (MAM), methyl 4-amino-2-ethoxybenzoate (MAE) and methyl-4-acetamidobenzoate (MAB).

Preparation of ETP imprinted microspheres by an oxidation-reduction initiating system

ETP imprinted microspheres were synthesized using precipitation polymerization. The template molecule (ETP, 0.5 mmol) was dissolved in 50 mL of acetonitrile and placed in a 100 mL flat-bottomed flask. Afterward, 3 mmol functional monomer (MAA, AM or 4-VP) was added. The mixture was sealed and incubated at 4°C for 24 h. Subsequently, the cross-linker (PETRA, 10 mmol, 1.886 mL) and the initiator (BPO, 0.032 mmol; DMA, 0.032 mmol) were added stepwise. The mixed solution was poured into a sonication bath for 5 min to dissolve the chemicals sufficiently, and then purged with nitrogen for 5 min to remove oxygen which inhibits the polymerization. Polymerization was performed in a water bath with the temperature being maintained at 25°C for 24 h. After reaction, the resulting particles were collected by centrifugation (6000 rpm, 5min). The template was then removed by centrifuging (6000 rpm, 5 min) with methanol containing 10% acetic acid (v/v) until no template could be detected from the washing solvent by HPLC. The polymeric particles were finally washed with acetone and dried in a vacuum chamber. Non-imprinted reference polymer (NIP) was synthesized under identical conditions except for omission of the template ETP [13].

Characterizing ETP imprinted microspheres

Study of the adsorption behaviour. Substrate recognition had been studied by static adsorption test. A 25 mg of MIP or NIP was placed into a 10mL plastic centrifuge tube and mixed with 5 mL of an ETP solution (0.5 mmol L^{-1}). After 24 h adsorption at 25°C, the substrate concentrations were quantified by calibration curve developed with HPLC at the concentrations of 0.01 mmol L^{-1}-0.1 mmol L^{-1} of ETP standard solutions, with 6 calibration levels. The different amounts of substrates bound to MIPs (Q, μg g^{-1}) were detected in triple and calculated by the following equation [14]:

$$Q = \frac{(C_{s_0} - C_s) \times V}{m} \quad (1)$$

Here, C_{s0} and C_s are the concentrations of substrates in the initial solution and in the supernatant after treatment for a certain period of time

Analytical Methods Accepted Manuscript

 This journal is © The Royal Society of Chemistry 2015

(mmol L^{-1}), respectively. V is the volume of ubstrate solution (mL), and m is the weight of the dry MIPs used (g).

The imprinting factor (IF) of the imprinted polymer was calculated by the following equation:

$$IF = \frac{Q_{MIP}}{Q_{NIP}} \quad (2)$$

Where Q_{MIP} and Q_{NIP} are the static adsorption amounts of MIP and NIP (μg g^{-1}), respectively.

Selective assessment. Selective assessment test was performed by choosing the ETP-imprinted microsphere with the highest IF value. The MIP (50 mg) was added into a plastic centrifuge tube containing 5 mL of 0.5 mmol L^{-1} ETP or a structurally related compound. After 24 h oscillation in a constant temperature air bath shaker at 25 °C, the mixtures were centrifuged at 15000 rpm for 15 min. Subsequently, the concentrations of the free molecules were detected by the HPLC, and the adsorptive parameter of selectivity index (SI) was calculated [15, 16].

$$SI = \frac{IF_{analyte}}{IF_{template}} \quad (3)$$

Where $IF_{analyte}$ and $IF_{template}$ are the IF values of MIP and NIP, respectively.

Isotherm and Scatchard analysis. Ten batches of 50 mg polymers were weighed into plastic centrifuge tubes and mixed with 5 mL acetonitrile solutions of ETP respectively (the ETP concentration varied from 0.1 mmol L^{-1}-1 mmol L^{-1}). In the constant temperature air bath shaker, the mixtures had been shaken for 24 h at 25 °C, and then centrifuged at 15000 rpm for 15 min. The resulting supernates were determined using the HPLC method. The obtained data were fitted by equation (4), and the isotherm was plotted based on the ETP concentrations in supernatants versus the amount of substrate bound to MIPs.

$$\frac{Q}{C} = \frac{Q_{max}}{K_D} - \frac{Q}{K_D} \quad (4)$$

K_D is the equilibrium dissociation constant, C is the free equilibrium concentration of ETP (mmol L^{-1}), and Q_{max} is the apparent maximum number of binding sites (μg g^{-1}).

Development of standard curve by CL assay

ETP imprinted microspheres (30 mg) were suspended in 1mL water containing 0.1% PVA. A 100 μL aliquot of this suspension was applied onto the inner surface of microplate wells and dried at 60°C for 30 min [17].

A volume of 50 μL of ETP solution was added into the well of the microtiter plate coated with the microspheres and adsorbed for 30 min. The plate was then rinsed thoroughly with ethanol. Subsequently, the chemiluminescent substrates of 50 μL TCPO, 50 μL H_2O_2 and 25 μL IMZ solutions were immediately added. After vortex shaking for 8s-10s, the light emitted was quantified using the Chemiluminescence Analyzer until it reached a plateau. The background value was obtained by imaging an equally sized region outside the region of interest and was subtracted from each measurement. Date acquisition and treatment were performed with the IFFL-D software. The standard curve was generated by plotting the average signal intensities obtained for ETP standard on the vertical (Y) axis versus the corresponding ETP concentrations on the horizontal (X) axis.

Determination of ETP in chicken muscle with a CCD camera

The chicken muscle samples were cut into pieces and homogenized, and ETP standard was spiked in the samples with the concentrations of 250 μg kg^{-1}, 500 μg kg^{-1} and 1000 μg kg^{-1}. An accurately weighed 5 g amount of the tissue was mixed with 20 mL acetonitrile in a centrifuge tube and 2 g anhydrous Na_2SO_4 added. After 10 min of vortex mixing, the mixture was centrifuged 5 min at the speed of 5000 rpm. Then the supernatant was filtered in a 100 mL conical flask, and the residue was extracted for 15 min in water bath by ultrasonic wave. Subsequently, the extracts were combined and evaporated at 35 °C under vacuum [18]. The dry residue was dissolved by 5% methanol-water, transferred in a 5 mL centrifuge tube, and added 3 mL n-hexane. Followed by a 10 min vortex mixing, the mixture was allowed the phases to separate into two layers, and the supernatant liquid was finally decanted. The same procedure was repeated. Then the residual layer was made up to 2 mL with 5% methanol-water, and the extracts were purified by a 3 mL solid phase extraction (SPE) column (Oasis® HLB). The SPE microcolumn was preconditioned with 3 mL methanol and 3 mL water, rinsed with 6 mL 10% acetonitrile-water, and eluted by 6 mL acetonitrile. The eluent was evaporated at 35 °C under vacuum.

ETP concentrations in chicken muscle were determined using the CL assay described above. The concentration of ETP in the real sample was calculated with the equation of the calibration curve obtained with the standard.

Results and discussion

Evaluation of imprinted microspheres

Adsorption parameters of ETP imprinted microspheres. Uniform MIP microspheres were readily obtained using precipitation polymerization when appropriate amounts of print molecule, functional monomer and cross-linker were utilized. The adsorption parameters of ETP MIPs are shown in Table 1. The highest IF polymer (P1) was synthesized with MAA and the cross-linker, which displayed the most specific recognition of ETP. The adsorption amounts of P1-M and P1-N were 8541.0 μg g^{-1} and 3321.5 μg g^{-1}, respectively.

Table 1 The adsorption capability and imprinting factor of ETP MIPs[a].

MIPs	Monomer	C_s (mmol L^{-1})	Q (μg g^{-1})	IF
P1-M	MAA	0.32	8541.0	2.57
P1-N	MAA	0.43	3321.5	
P2-M	AM	0.39	5219.5	1.83
P2-N	AM	0.44	2847.0	
P3-M	4-VP	0.42	3796.0	1.60
P3-N	4-VP	0.45	2372.5	

[a] Q, adsorption capacity, $Q = (C_{s0}-C_s)\times$(loading solution volume [mL]/adsorbent mass [g]), C_{s0} and C_s represent concentrations of the substrates in the initial solution and in the supernatant after treatment for a certain period of time (mmol L^{-1}), respectively. IF, imprinting factor, $IF = Q_{MIP}/Q_{NIP}$, Q_{MIP} and Q_{NIP} are the static adsorption amounts of MIP and NIP (μg g^{-1}), respectively.

Analytical Methods Accepted Manuscript

Fig. 2 shows the relationship between adsorption capacity and adsorptive time. The adsorption amounts of P1 increased most quickly in the period of 0 h-2 h, and the saturated adsorption was observed after 4 h.

Inventory ratio has a dramatic effect on ETP imprinting process. The molar ratio between the functional monomer and template has been found to be important with respect to the number and quality of MIP recognition sites. Lower ratios between template and functional monomer can result in a relatively decreased yield of high-affinity binding site, and higher ratios often promote the non-specificity of MIPs. Moreover, according to the reports, the high performance polymers were obtained when the ratio between functional monomer and cross-linker was 1:5 [13].

FT-IR spectra. Fig. 3 provides structural information about the molecular interactions between ETP and MAA. The spectrum of NIP was similar to MIP absorption bands at the same wavenumber but with less absorbance. Due to H-bond formation between the C=O group of MAA and the O-H group of ETP, the stretching vibrations of C=O and O-H are shifted in different extent. The FT-IR spectra of the polymers are similar, but the locations, strengths and widths of the vibrational peaks for the C=O and O-H groups in MAA are significantly different. In the FT-IR spectrum of MIP, the stretching vibrations of O-H (3500 cm^{-1}-3400 cm^{-1}) and C=O (1760 cm^{-1}-1700 cm^{-1}) were the characteristic absorption of COOH of MAA. These peaks moved slightly when adding an ETP (template) molecule in the imprinting system, which indicated that H-bonds formed between these molecules. Moreover, a comparison between the FT-IR spectra found that the intensity of some signals in the range of 3000 cm^{-1}-4000 cm^{-1} was lower in the case of NIP than in MIP, or some signals were slightly shifted. This can be attributed the fact that the multiple H-bond interactions of functional monomers were disrupted after the addition of template in the imprinting process.

Selectivity of ETP imprinted microspheres. The selectivity of an imprinted polymer is of major importance for a successful analytical application. It is governed mostly by the equilibrium that exists at the polymer-solution interface, and can be determined experimentally by calculating the SI values. The resulting data reflect the ability of microspheres to differentiate ETP from species that interfere in the analysis. It is suggested that the lower SI value implies the higher specificity. The imprinting parameters of all the substrates are presented

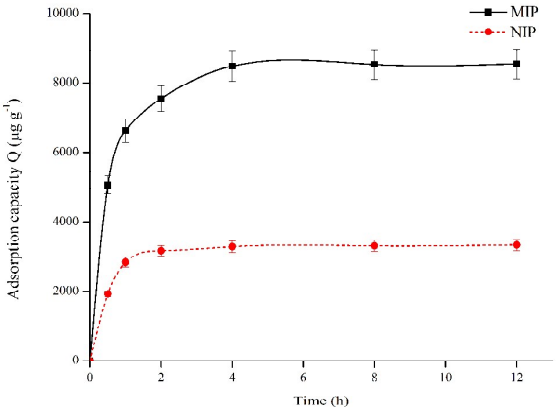

Fig. 2 The kinetic adsorption curves of ETP microspheres.

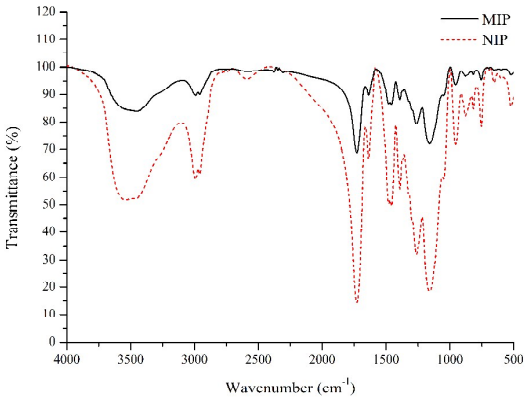

Fig. 3 The infrared spectra of NIP and MIP.

in Table 2. ETP-imprinted microsphere had a high affinity for the template. However, as for the structurally related compounds, the binding specificity toward other substrates was relatively low. It is estimated that the SI values were no more than 0.7 [19].

Affinity analysis. Fig. 4a shows the binding isotherms for ETP on the MIP and NIP. The binding amounts increased gradually with the ETP concentration in the initial solution. It can be seen that the amount of ETP bound to the MIP was more than that to the NIP, which can be ascribed to the imprinting effect of template.

The obtained data were plotted according to the Scatchard equation. Fig. 4b shows two distinct sections within the plot, which indicated that there were two kinds of the binding sites in the MIP, one was high-affinity site (K_{D1} = 23.92 μg L^{-1}, Q_{max1} = 8808.28 μg g^{-1}), and the other was low-affinity site (K_{D2} = 77.82 μg L^{-1}, Q_{max2} = 14043.90 μg g^{-1}). However, there was only the low-affinity site in NIP (K_D = 9.19 μg L^{-1}, Q_{max} = 3632.77 μg g^{-1}).

Micrographs of ETP imprinted microspheres. Fig. 5 shows the surface morphology of ETP MIP (a) and NIP (b) microspheres, respectively. Based on the result, it can be deduced that the template has a great influence on the size and appearance of the imprinted microspheres.

Table 2 Test for selectivity assessment of ETP microspheres [a].

MIPs	Substrates	C_s (mmol L^{-1})	Q (μg g^{-1})	IF	SI
MIP-1	ETP	0.32	8541.00	2.57	1.00
NIP-1	ETP	0.43	3321.50		
MIP-1	MAB	0.36	4232.48	1.56	0.60
NIP-1	MAB	0.41	2720.88		
MIP-1	MAM	0.41	3261.42	1.50	0.58
NIP-1	MAM	0.44	2174.28		
MIP-1	MAE	0.37	5075.72	1.63	0.63
NIP-1	MAE	0.42	3123.52		

[a] Q, adsorption quantity, $Q = (C_{s0}-C_s) \times V/m$, C_{s0} and C_s are the concentrations of substrates in the initial solution and in the supernatant after treatment for a certain period of time, respectively. V is the volume of substrate solution and W is the weight of the dry MIPs used. IF, imprinting factor, $IF=Q_{MIP}/Q_{NIP}$, Q_{MIP} and Q_{NIP} are the static adsorption amounts of MIP and NIP (μg g^{-1}), respectively. SI, selectivity index, $SI=IF_{analyte}/IF_{template}$, $IF_{analyte}$ and $IF_{template}$ are the imprinting factors of MIP and NIP, respectively.

Analytical Methods Accepted Manuscript

This journal is © The Royal Society of Chemistry 2015

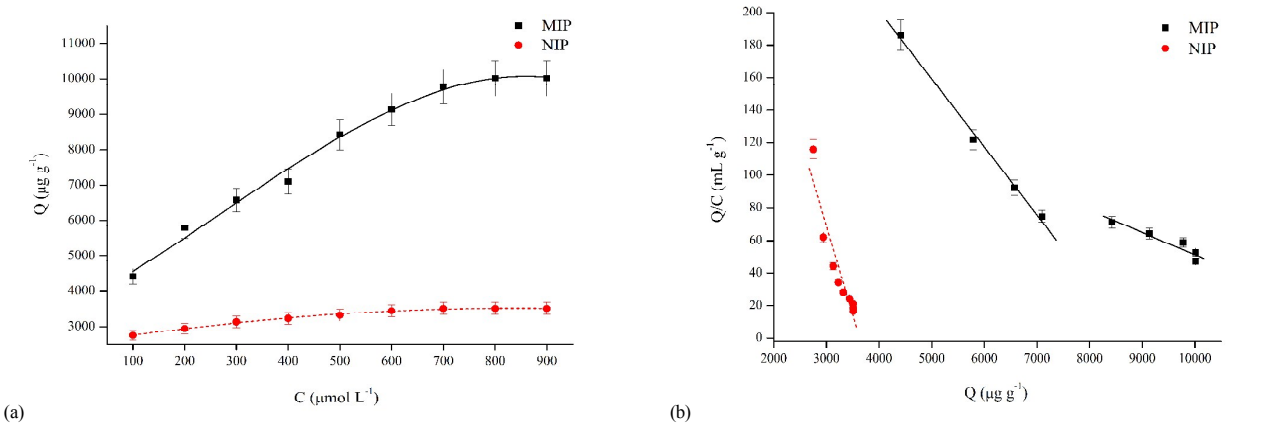

Fig. 4 Isotherm (a) and Scatchard plots (b) of ETP adsorption on MIP and NIP.

The porous solvent plays an essential role that influenced the size, surface morphology and distribution of pores in the polymer. To a great extent, all these properties depend on the solubility of the growing polymer chains in the solvent. Specifically speaking, the volume, viscosity and polarity of solvent affect the polymer structure and micrograph without exception [20]. Above all, the high polarity solvent can interfere with the bonding formation of template and binding sites, which leads the binding amounts of polymers to decrease. Besides, the high viscosity and small volume of solvent would be more inclined to prepare large-sized and high-polymerization-degree MIPs. For example, the large diameter microspheres were polymerized by using methanol instead of acetonitrile in the preliminary test.

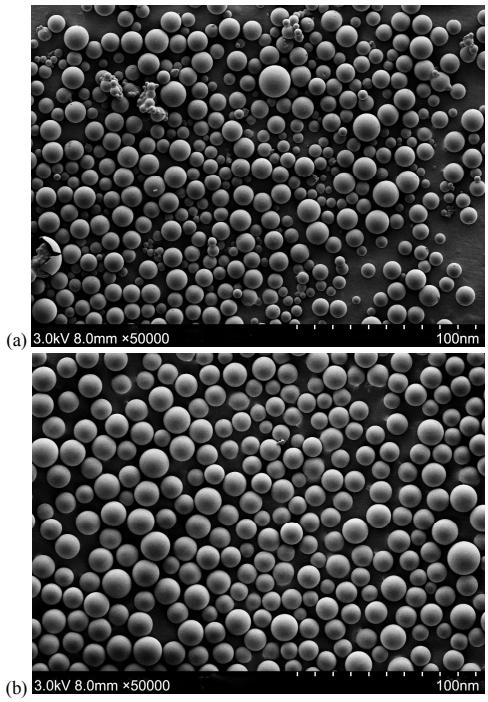

Fig. 5 SEM image of ETP MIP (a) and NIP (b) microspheres at 50000 magnification.

In addition, the average diameter of NIP microsphere was a little larger than that of MIP microsphere, suggesting that the template had an important influence on the particle growth during the polymerization. This is not surprising given that the template and MAA could form hydrogen bonds, which would affect the growth of the cross-linked polymer nuclei to result in smaller polymer beads [21].

Thermal stability. To investigate the thermal stability of the ETP microspheres, the differential scanning calorimetry (DSC) was carried out between 25 °C and 250 °C under a nitrogen atmosphere. The DSC curve of the polymer is shown in Fig. 6. With the temperature increasing, the endotherm increased gradually. It can be seen that the endothermic peaks of NIP and MIP appeared at the temperatures of 79.4 °C and 65.7 °C, respectively. The occurred peaks can be defined as the phase transition process. However, the addition of template in the preparation of MIP led to low cross-linking degree and low phase transition temperature. After passing the maximum endothermic peaks, each DSC curve showed a slight slope relative to a flat baseline, reflecting the endotherm was decreased or even disappeared. When the temperature was above 200 °C, an exothermic process occurred for the polymers, suggesting different levels of decomposition appeared. The DSC plot indicates that the MIPs are sufficiently stable in laboratory and on-site detections.

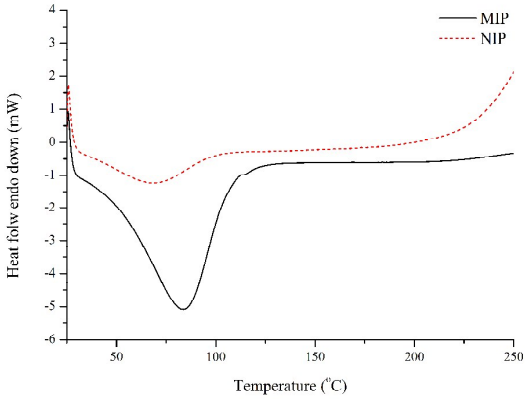

Fig. 6 The DSC spectra of ETP MIP and NIP microsphers.

Analytical Methods Accepted Manuscript

Optimization of the CL imaging conditions

The CL imaging assay was developed by optimizing the solvent and concentrations of TCPO, H_2O_2 and IMZ used in the determination. Several solvents, namely methanol, acetonitrile, acetone and ethyl acetate, were investigated. It is believed that the low polar solvent was favorable for the recognition of ETP with the microsphere. Considering the solubility and the influence of swelling process, acetonitrile was finally chosen as the solvent. Fig. 7 shows the light intensity-time profiles for the PO-CL system of ETP with varying concentrations of TCPO. It can be seen in the Fig., the CL intensity enhanced gradually as the TCPO concentration increases. In view of the limited solubility of TCPO, a final concentration of 5 mmol L^{-1} was selected as the optimum. Fig. 8 shows the typical response curves for the PO-CL system of ETP in the presence of varying concentration of H_2O_2. Keeping the concentrations of TCPO (5 mmol L^{-1}) and ETP (1 μg mL^{-1}) constant, and adjusting correspondingly the H_2O_2 concentration from 0.2 mmol L^{-1} to 4 mmol L^{-1}, the CL intensity increased initially as the H_2O_2 concentration increased. The high CL background was observed when the H_2O_2 concentration was higher than 1 mmol L^{-1}. It makes no sense for overhigh H_2O_2 concentration. Therefore, 1 mmol L^{-1} H_2O_2 was determined as the optimal concentration.

As one of the most efficient catalysts for TCPO reaction, imidazole (IMZ) has been used successfully in the CL analysis [22]. Under the constant concentrations of H_2O_2 (1 mmol L^{-1}), TCPO (5 mmol L^{-1}) and ETP (1 μg mL^{-1}), the response of the PO-CL system was measured in the presence of varying concentration of IMZ. The resulting CL intensity–time plots are shown in Fig. 9 for a temperature of 25 °C. As shown in the Fig., with the concentration of IMZ increasing, the maximum signal intensity increased, and the time to reach the maximum signal decreased. However, the profile area decreased when the IMZ concentration was higher than 5 mmol L^{-1}. Therefore, 5 mmol L^{-1} was chosen as the final optimum IMZ concentration.

The exposure time was also investigated from 5 s to 200 s under the optimal conditions described above. As the exposure time prolonged, the imaging intensity increased, however, the resolution reduced accordingly. Therefore, taking sensitivity, resolution and analytical efficiency into consideration, an exposure time of 50 s was selected as the optimum in the detection.

After immobilizing the microspheres with different concentrations of PVA, the influence of PVA concentration on binding of ETP to the imprinted microspheres (750 μg per well) was investigated. Fig. 10 shows the imaging intensities from the experiment in which the PVA concentrations were varied. Relative signal was plotted on the vertical axis against PVA concentration on the horizontal axis. As the PVA concentration increased, the imaging intensity increased initially but then decreased gradually. Moreover, the maximum signal was observed at 0.1% PVA. This can be illustrated by a PVA layer which formed around the microspheres and masked some binding sites on the polymer. However, the immobilized layer would be unstable when the PVA used in this work was lower than 0.1%. Therefore, 0.1% PVA was used for immobilization of microsphere on the plate.

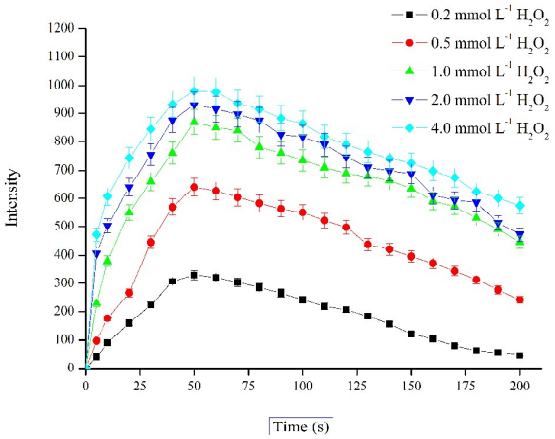

Fig. 8 CL intensity-time profiles of varying H_2O_2 concentrations with 5 mmol L^{-1} TCPO, 5 mmol L^{-1} IMZ and 1 μg mL^{-1} ETP at 25 °C.

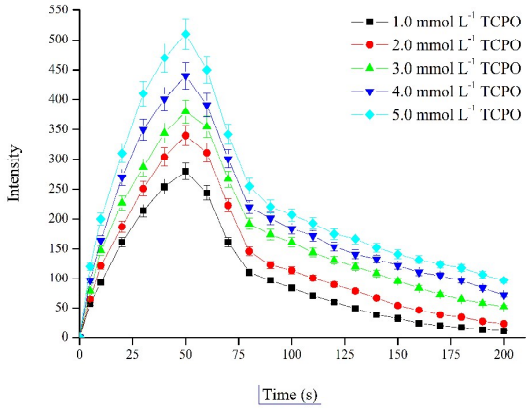

Fig. 7 CL intensity-time profiles of varying TCPO concentrations with 1 μg mL^{-1} ETP, 5 mmol L^{-1} IMZ and 1 mmol L^{-1} H_2O_2 at 25 °C.

Optimization of the absorption conditions

Due to the swelling effect of polymer, ETP imprinted microspheres were exposed to the same conditions as those used for polymerization. Both imprinting and rebinding experiments were performed in acetonitrile. The relationship between CL intensity and adsorption time within the range of 5 min-60 min was investigated using 1 mmol L^{-1} H_2O_2, 5 mmol L^{-1} TCPO and 1 μg mL^{-1} ETP in a microtiter plate which was coated with the

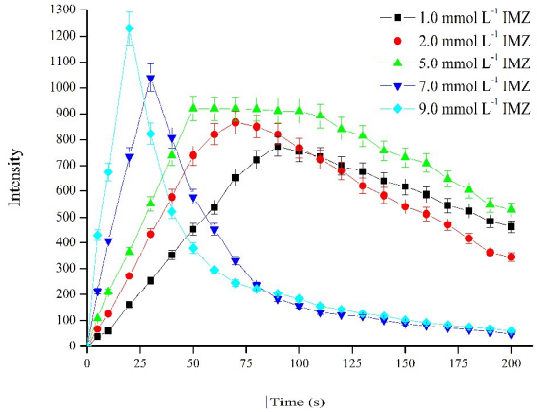

Fig. 9 CL intensity-time profiles of varying IMZ concentrations with 1 mmol L^{-1} H_2O_2, 5 mmol L^{-1} TCPO and 1 μg mL^{-1} ETP at 25 °C.

Analytical Methods Accepted Manuscript

This journal is © The Royal Society of Chemistry 2015

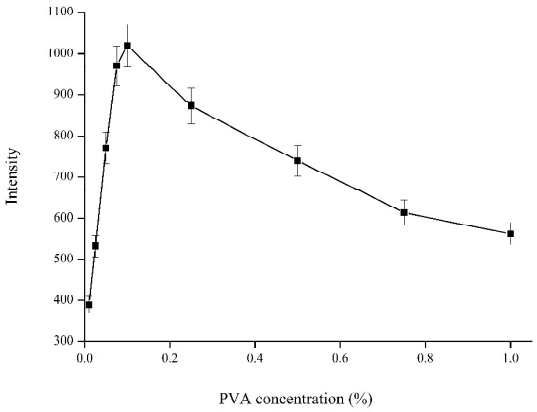

Fig. 10 Effect of PVA concentration on CL imaging intensity.

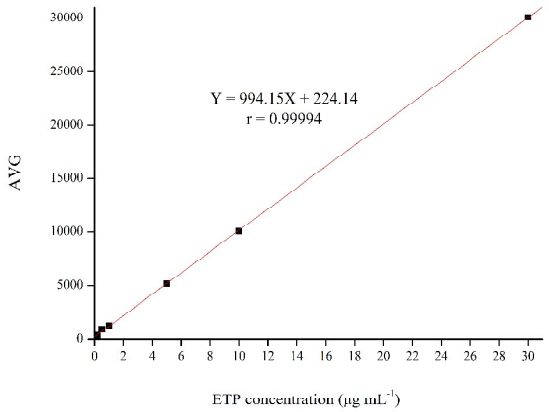

Fig. 12 Corresponding imaging intensity (AVG) for the different ETP concentrations with the imprinted microspheres.

microspheres by 0.1% PVA. As can be seen in Fig. 11, the CL intensity raised as the adsorption time increased to 30 min. When the time was over 30 min, the intensity remained constant and the non-specific adsorptions increased. Therefore, 30 min was chosen as the adsorption time for this method. However, it should be mentioned that for the analysis of a sample with trace ETP, the sensitivity could be improved by increasing the adsorption time.

Analytical characteristics of ETP standard curve

With the optimized conditions, a microtiter plate-based imaging assay was developed. As can be seen in Fig. 12, the imprinted polymer has sensitive response to the template. The standard curve of ETP was linear over a concentration range of 0.1 μg mL^{-1}-30 μg mL^{-1}. It can be described by the linear regression equation (Y=994.15X+224.14, r=0.9999), where Y is the relative CL imaging intensity (AVG) and X is the ETP concentration (μg mL^{-1}).

Interference study

In a real sample, the analyte (1 μg mL^{-1} ETP) will be investigated in the presence of interferents. Although they have no significant effect on the intensity, there is a strong possibility that the synchronous signal is suppressed or enhanced by them. The tolerable limit of a foreign species was taken as a relative error less than 5%. Many metal ions could strongly catalyse the CL reaction and could interfere with ETP detection by use of this CL system. The results were summarized in Table 3. From the Table it could be seen that the influences of anionic ions on the CL intensity were slight, most cationic ions, 1500-fold Na^+, K^+, Ca^{2+}, Mg^{2+}, Zn^{2+}, Pb^{2+}, 1200-fold Ba^{2+}, Al^{3+}, and 900-fold Co^{2+}, Cu^{2+}, have no influence on the determination of 1 μg mL^{-1} ETP. Other substances existing in chicken muscle, such as glucose, acetic acid, citric acid, tartaric acid, glycine, glutamic acid and asparagic acid, were examined to assess their interferences in the detection [23]. The tolerable concentration ratios of these coexisting compounds were higher than 5000. Thus, the proposed procedure is able to sense ETP in the presence of several possible interferences with high selectivity.

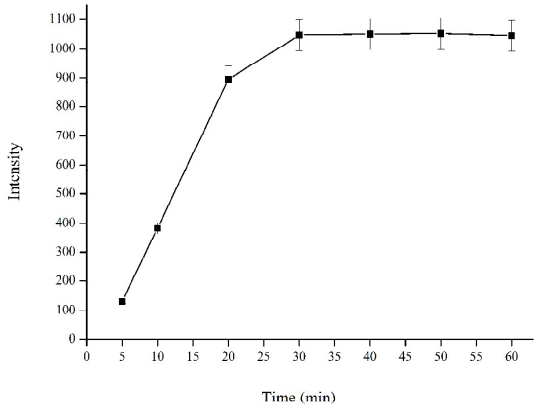

Fig. 11 Effect of adsorption time on CL imaging intensity.

CL assay of ETP in chicken muscle

The application of this method was validated by detecting the recovery

Table 3 The tolerable ratios of interfering substances to ETP in chicken muscle samples.

Substances	With NIP	With MIP
Glucose	730	10000
Acetic acid	870	9700
Citric acid	760	8000
Tartaric acid	650	7800
Glycine	750	7700
Glutamic acid	800	7400
Asparagic acid	760	5900
Na^+	400	1500
K^+	400	1500
Ca^{2+}	430	1500
Mg^{2+}	390	1500
Zn^{2+}	390	1500
Pb^{2+}	410	1500
Ba^{2+}	350	1200
Al^{3+}	350	1200
Co^{2+}	330	900
Cu^{2+}	330	900

Analytical Methods Accepted Manuscript

of known amounts of ETP in the samples of chicken muscle. Samples were measured in triplicate using 96-well plates. Recovery and relative standard deviation (R.S.D.) at each spiked concentration were recorded in Table 4. After detecting 30 blank samples, the limit of detection (LOD) was calculated as the concentration of analyte that results in the response equal to three standard deviations of the background noise. The LOD for ETP was 14.7 μg kg^{-1}. Furthermore, the limit of qualification (LOQ) was defined if only the recoveries and variability could meet the requirements of CL determination. Its value was determined as 20.4 μg kg^{-1} for chicken muscle.

Although the molecular imprinting CL method (MI-CL) could be used in ETP residue analysis, the variation was higher than the CL method based on biological antibody. This can be attributed to the surface inhomogeneity of microplate and microsphere, the imprecision of recognition, the monotony of the repetitive polymer structure, and the rigid recognition cavity which lacked induced fit interaction and the flexible docking process. These characteristics were just different from the exact identification of biological antibody. But the greatest strength of the MI-CL is the simplification for MIPs preparation which will promote its application in the analysis of residues.

Influence of matrix interference on assay performance

Matrix interference on veterinary residue analysis is a common problem in CL detection. As described in previous reports, the simplest approach to avoid the matrix interference is to properly dilute sample extract with water or buffer [24]. However, the sensitivity of the MI-CL method may be reduced. The problem will also be resolved by giving appropriate sample pretreatment such as SPE, liquid-liquid extraction, or column chromatography etc. in the determination [25]. But these methods as described above do not show the selectivity of the target component. According to the report, it has been proved to be effective and practicable by using molecular imprinting SPE columns for the selective extraction of analyte from heterogeneous biological matrices [13]. Moreover, the specificity of the SPE procedure on MIP columns allowed the further analysis of the ETP residue by applying the MI-CL method. It is suggested that the application of molecular imprinting SPE column in routine analysis could be a real tool to improve analytical specificity [26].

The procedures for reducing the interferences include the extraction and clean-up steps. Generally, the extraction of ETP from real samples has been performed with organic solvents, such as chloroform, methylene chloride, acetone, acetonitrile or ethyl acetate etc. [18]. Some of them also denature the sample protein, which results in a cleaner extraction and helps release any drug residues bound to proteins. In this study, it was found that the use of acetonitrile in extraction could improve the recovery and purification of real samples. For the clean-up of ETP, the SPE column showed robust repetition and high recovery efficiency.

Table 4 Recovery and precision data for spiked ETP in chicken muscle samples.

Sample	Spiked concentration (μg kg^{-1})	Found concentration (μg kg^{-1})	Recovery (%)	R.S.D. (%)
1	250	249.5±1.3	99.80	3.4
2	500	500.7±0.9	99.94	2.9
3	1000	1001.1±0.7	99.98	1.7

Conclusions

The CL imaging assay based on ETP imprinted microsphere has been developed for the first time. It will enable simultaneous measurement and high-throughput screening of fluorescent compounds in a large number of samples. This method was validated by calculating the recoveries of known amounts of ETP in real samples. It has shown a great potential application prospect in measurement of other native fluorescent compounds and fluorescent derivatized compounds which could be detected in the PO-CL system. Furthermore, this system may be particularly useful in cases where biological antibodies are difficult to obtain or where long-term stability and cost of the assay is of importance. Even though this assay is still less sensitive than some recently developed biological antibody-based assays, it is believed that the findings would increase the potential of MIPs for bionic immunoassay-type applications, and the present approach or similar ones could provide useful analytical system in many instances [27].

Acknowledgements

This study was supported by National Natural Science Foundation of China (No. U1504330), Doctoral Research Initiation Grant from Henan University of Science and Technology (No. 09001609), National Student Research Training Program of Ministry of Education of PR China (No. 201310464007), Youth Science Foundation of Henan University of Science and Technology (No. 2013QN021), Innovative Capacity Cultivating Foundation in Natural Science of Henan University of Science and Technology (No. 2014ZC X021) and Key Science and Technology Program of Educational Comm- ission of Henan Province, PR China (No. 14B550015).

References

1. J. J. Nasr and S. Shalan, *Luminescence*, 2014, **29**, 1188-1193.
2. Veterinary Drug MRL Database. https://vetdrugs.globalmrl.com/results.cfm (accessed on 27 April 2015).
3. R. L. Smallidge, Jr., *J. Assoc. Off. Anal. Chem.*, 1978, **61**, 561-563.
4. R. H. M. M. Granja, A. M. Montes Nino, R. A. M. Zucchetti, R. E. Montes Nino and A. G. Salerno, *J. AOAC Int.*, 2008, **91**, 1483-1487.
5. J. J. Nasr, S. Shalan and F. Belal, *Food Anal. Methods*, 2013, **6**, 1522-1528.
6. K. Pietruk, M. Olejnik, P. Jedziniak and T. Szprengier-Juszkiewicz, *J. Pharm. Biomed. Anal.*, DOI: http://dx.doi.org/10.1016/j.jpba.2015.03.019, In press.
7. L. Clarke, M. Moloney, J. O'Mahony, R. O'Kennedy and M. Danaher, *Food Addit. Contam. Part A Chem. Anal. Control Expo. Risk Assess.*, 2013, **30**, 958-969.
8. L. Wang and Z. Zhang, *Anal. Chim. Acta*, 2007, **592**, 115-120.
9. Akimitsu Kugimiy and H. Takei, *Anal. Chim. Acta*, 2008, **606**, 252-256.
10. L. Wang and Z. Zhang, *Sens. Actuators B Chem.*, 2008, **133**, 40-45.

Analytical Methods Accepted Manuscript

 This journal is © The Royal Society of Chemistry 2015

11. P. Chang, Z. Zhang and C. Yang, *Anal. Chim. Acta*, 2010, **666**, 70-75.
12. A. G. Mohan and N. J. Turro, *J. Chem. Educ.*, 1974, **51**, 528.
13. A. R. Khorrami and M. Edrisi, *Sep. Sci. Technol.*, 2010, **45**, 404-412.
14. H. Yavuz, V. Karakoc, D. Turkmen, R. Say and A. Denizli, *Int. J. Biol. Macromol.*, 2007, **41**, 8-15.
15. Y. Liu, X. L. Liu and J. D. Wang, *Chin. J. Anal. Chem.*, 2003, **31**, 1202-1206.
16. Y. Jin, Y. Zhang, Y. Zhang, J. Chen, X. Zhou and L. Bai, *J. Chem.*, 2013, **2013**, 9.
17. L. Wang, Z. Zhang and L. Huang, *Anal. Bioanal. Chem.*, 2008, **390**, 1431-1436.
18. H. W. Sun, L. F. Ai and F. C. Wang, *Chromatographia*, 2007, **66**, 333-337.
19. F. T. C. Moreira, R. A. F. Dutra, J. P. C. Noronha, J. C. S. Fernandes and M. G. F. Sales, *Sens. Actuators B Chem.*, 2013, **182**, 733-740.
20. S. T. Wei, M. Jakusch and B. Mizaikoff, *Anal. Chim. Acta*, 2006, **578**, 50-58.
21. X. Zhou, W. Y. Li, X. W. He, L. X. Chen and Y. K. Zhang, *Sep. Purif. Rev.*, 2007, **36**, 257-283.
22. J. Kang, L. Han, Z. Chen, J. Shen, J. Nan and Y. Zhang, *Food Chem.*, 2014, **159**, 445-450.
23. Q. Zhang, J. Li, T. Ma and Z. Zhang, *Food Chem.*, 2008, **111**, 498-502.
24. A. Posyniak, J. Zmudzki and J. Niedzielska, *Anal. Chim. Acta*, 2003, **483**, 61-67.
25. E. Watanabe, H. Eun, K. Baba, T. Arao, Y. Ishii, S. Endo and M. Ueji, *Anal. Chim. Acta*, 2004, **521**, 45-51.
26. C. Y. He, Y. Y. Long, J. L. Pan, K. Li and F. Liu, *J. Biochem. Biophys. Methods*, 2007, **70**, 133-150.
27. I. Surugiu, B. Danielsson, L. Ye, K. Mosbach and K. Haupt, *Anal. Chem.*, 2001, **73**, 487-491.

Analytical Methods Accepted Manuscript

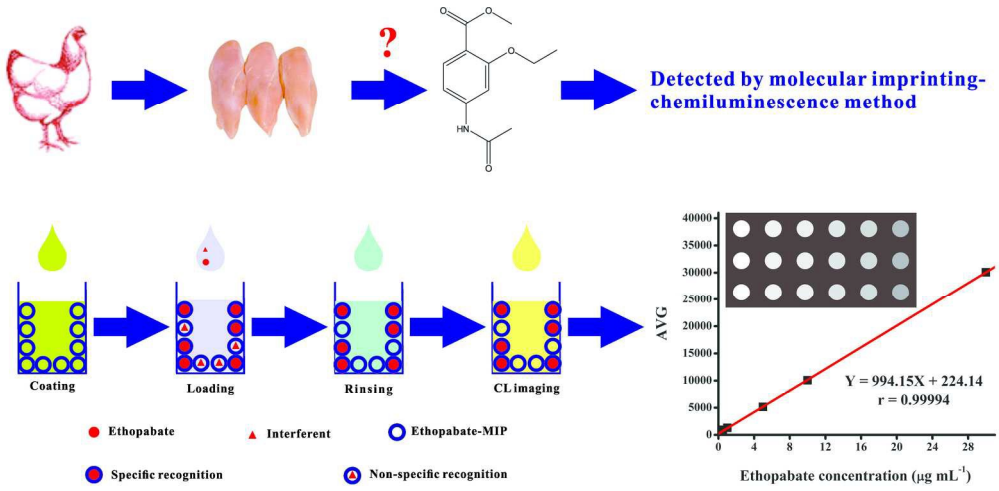

194x93mm (300 x 300 DPI)

Analytical Methods Accepted Manuscript